

Analysis of climate trends and change point detection in Upper Middle Olifants catchment, South Africa

Mesfin Reta Aredo^{1,*}, Megersa Olumana Dinka¹

¹ Department of Civil Engineering Sciences, Faculty of Engineering and the Built Environment, University of Johannesburg, Johannesburg, South Africa

Abstract

Climate variability poses a pressing shift to the hydrological cycle and diminishing water resources availability. This shift is a prevalent challenge for day-to-day activities in the Olifants River, South Africa. This study assessed rainfall, minimum and maximum temperature variability, trend analysis, and change point detection in the Olifants River using numerous statistical analysis methods, such as coefficient of variation, Kurtosis, skewness, Pettitt, Buishand, von Neumann, Standard normal homogeneity test (SNHT), Mann-Kendall, and Sen's slope tests for the period from 1988 to 2014. The results showed that annual rainfall in most stations had moderate variation, while limited stations were negatively skewed and not normally distributed. Most of the stations, such as X1E003, B5E004, and B1E003, showed less variability ($CV < 20$), while the rest of the stations showed moderate variation ranges ($20 < CV < 30$) for rainfall datasets. The results of kurtosis and skewness ranged from -0.41 to 1.10 and -0.12 to 0.46 for rainfall; -0.03 to 0.92 and -0.61 to -0.17 for maximum temperature; and 0.24 to 1.61 and -0.18 to 0.14 for minimum temperature, respectively. Furthermore, the majority of stations were negatively skewed for annual maximum and minimum temperatures. Unexpectedly, the homogeneity tests for annual rainfall and maximum temperature depicted favorable results, while a few stations were found to be non-homogeneous for minimum temperature. Specifically, the trend analysis indicators such as Kendall's tau, S, p -value and Sen's slope showed ranges from -0.03 to 0.15, -11 to 53, 0.28 to 1.0, and -1.95 to 4.98 for rainfall; 0.08 to 0.15, 29 to 51, 0.30 to 0.56, and 0.009 to 0.025 for maximum temperature; and 0.13 to 0.24, 45 to 85, 0.08 to 0.36, 0.01 to 0.014 for minimum temperature, respectively. The trend analysis results revealed that the highest percentage of stations were showing an increasing trend, while the magnitude varied slightly for annual rainfall, maximum, and minimum temperatures. Sustainable and innovative climate variability mitigation measures must be initiated to reduce the effects of variability in agricultural productivity and environmental changes. Future researchers can investigate the effects of natural and anthropogenic activities on water resources and their implications for water availability.

Keywords: Change Detection, Homogeneity, Mann-Kendall, Sen's Slope, Trend Analysis

Article Type: Research Article

*Corresponding Author, E-mail: mesfinreta.mr@gmail.com

Citation: Aredo, M. R., & Dinka, M.O. (2025). Analysis of climate trends and change point detection in Upper Middle Olifants Catchment, South Africa. *Water and Soil Management and Modelling*, 5(Special Issue: Climate Change and Effects on Water and Soil), 199-214.

doi: 10.22098/mmws.2025.18183.1656

Received: 25 August, Received in revised form: 12 September 2025, Accepted: 21 September 2025, Published online: 23 September 2025

Water and Soil Management and Modeling, Year 2025, Vol. 5, Special Issue, pp. 199-214.

Publisher: University of Mohaghegh Ardabili

© Author(s)



1. Introduction

Water occurs under natural phenomena and covers a diverse hydrological cycle by changing from one state to another (Thapa et al., 2017). Furthermore, the hydrological water balance was affected due to rising anthropogenic and natural activities that may trigger hydrological extremes and undermine water availability (Tefera, 2017; Wakigari, 2017; Ayivi & Jha, 2018). The river is one of the main pillars of the hydrological component, which requires a comprehensive and sustainable development plan to develop, govern, manage, and regulate water resources for economic growth (Makungo et al., 2010; Jung et al., 2017; Pathak et al., 2019). Water is one of the scarce resources and has to be utilized optimally for the sustainable development of any country (Pathak et al., 2019). Recently, water resources have been extracted extensively to fulfil the drastically increasing water demand caused by rapid population growth and urbanization (Igibah & Tanko, 2019; Teshome et al., 2020). Water shortage is becoming a challenge on both local and global scales, while it is a significant pillar in achieving the UN's 2030 agenda (Aredo et al., 2024b). Water resources availability is challenged due to erratic climate patterns and anthropogenic activities (Loliyana & Patel, 2018; Aredo et al., 2023a). Climate change and variability are driving factors for vulnerabilities of hydrological extremes and changing water resources availability (Singh et al., 2021). Climate variability must be examined before conducting any hydrological investigation and development. For instance, if rainfall variability increases in the region, this may reduce surface runoff due to the probability of high infiltration capacity or increasing evapotranspiration (Zhao et al., 2013).

In different parts of the world, trend analysis findings showed varied rainfall trends (Bartels et al., 2019; Gao et al., 2020). The temperature records in the Black Volta basin show an increasing trend, while the upstream region in annual rainfall and streamflow showed declining trends (Abungba et al., 2020). Urbanisation, land degradation, and climatic factors might all contribute to a rising streamflow trend (Tadese et al., 2019). The temperature and streamflow were rising substantially in the Blue Nile basin, while

there was no significant trend in annual rainfall (Tekleab et al., 2013; Abera & Abegaz, 2020). Africa was increasingly dealing with the challenges of unpredictable rainfall patterns and significant swings in water resources due to the continent's skyrocketing water demands and variability (Aredo et al., 2023b; Aredo et al., 2024a). Africa's climate variables, such as rainfall, potential evapotranspiration, and temperature, fluctuate considerably (Tekleab et al., 2014; Cherinet et al., 2019; Tadese et al., 2019). Rainfall fluctuation with humid to arid climatic zone ranges, gentle terrain, and spatio-temporal hydrogeological variability will affect agricultural productivity (Nannawo et al., 2022). Climate variability analysis will produce insights into rainfall, temperature, and hydrology (Shahid & Rahman, 2021). Additionally, climate variability impacts the frequency and severity of extreme climatic events (Tehrani et al., 2019; Singh et al., 2021). Hydrological extremes were becoming prevalent across Africa, while flood-induced hazards have been underestimated in areas with less annual rainfall (Erena & Worku, 2019). Increasing temperature and rainfall variability affect small-scale farmers' agricultural production (Alashan, 2020; Nasir et al., 2021). The study's findings in South Africa's Limpopo River Basin depict increasing rainfall and maximum temperature trends, while the minimum temperature declined (Mosase & Ahiablame, 2018). Furthermore, in South Africa, the climate variability and trends were observed in numerous areas such as the Rietspruit sub-basin (Banda et al., 2021), Limpopo Province (Adeola et al., 2019), and Upper Karoo (Harmse et al., 2021). Climate variability, changes, and trends were noticed in the study area, with a limited level of understanding in the literature review in the Olifants River basin, a basin instrumental for South African (Gauteng, Mpumalanga, and Limpopo provinces) and Mozambique (Nkhonjera, 2017; Nkhonjera et al., 2021). If the country's development relies heavily on rain-fed agriculture, minimal rainfall fluctuation will affect agricultural productivity (Gedefaw et al., 2018; Mulugeta et al., 2019; Gonfa et al., 2022). Understanding hydro-climate trends at the basin or watershed levels is necessary for sustainable water resources

management and development (Bai et al., 2015; Sinha et al., 2018; Shahid & Rahman, 2021; Solaimani et al., 2021; Gonfa et al., 2022). Also, several studies were conducted on understanding climate variability, change detection, and trend analysis (Bailey et al., 2016; Bushira & Hernandez, 2019; Aredo et al., 2021a; Aredo et al., 2021b). Most studies were conducted on trend and variability analysis using 20 years of historical climate datasets, a limited period for comprehensive analysis (Shahid & Rahman, 2021).

The climate variability analysis will enhance agricultural productivity, water resource development, and management. The study area faces challenges due to climate variability, which demands a comprehensive evaluation of variability, change detection, and historical climate data trends. The most frequently used techniques for examining climate variability, change detection, and trend analysis were the coefficient of variation, Kurtosis, skewness, Pettitt, Buishand, von Neumann, SNHT, Mann-Kendall, and Sen's slope tests (Fentaw et al., 2019; Gulakhmadov et al., 2020; Nannawo et al., 2022). However, little attention has been paid to studies on change detection, climate variability, and trend analysis in the Olifants River basin using climate time series datasets and statistical analysis tools, which might be insightful to understanding hydro-climate variables across the basin. There is limited understanding of the variability and trend of the historical rainfall and temperature datasets for the greater Olifants River basin (Nkhonjera, 2017). This study is unique in comprehensively evaluating climate variables variability in the less studied Olifants River basin using numerous techniques from 1988 to 2014. This study aims to examine climate variability, change detection, and trend analysis using numerous statistical analysis techniques in the Olifants River, South Africa.

2. Materials and Methods

2.1. Study Area

The Upper-Middle Olifants Catchment (UMOC) lies between 24° 38' 53" and 26° 37' 45" S latitude and 28° 02' 56" and 29° 59' 22" E longitude

(Figure 1). The topography ranges from 823 m in the lower reach to 1868 m above mean sea level (m.a.s.l). The study area has been facing various annual rainfall and temperature variability. For instance, the annual precipitation is mainly received during the summer season, which falls within the 600 to 800 mm (Nkhonjera et al., 2021). The mean annual temperature in the study area varied considerably with changing topography and land cover (Nkhonjera, 2017; Nkhonjera et al., 2021). UMOC is located in South Africa's north-eastern areas and is a major tributary of the Limpopo River (Nkhonjera, 2017; Olabanji et al., 2020).

2.2. Data analysis

Climate datasets such as daily rainfall, maximum and minimum temperature were received from the South African Weather Service from 1988 to 2014, for each meteorological station presented in Figure 1. The missing daily climate datasets were filled using the inverse distance weight (IDW). The IDW technique computes the average value for the ungauged station using records from nearby weighted stations (Hadi & Tombul, 2018; Pirani & Modarres, 2020). Furthermore, the variability of the climatic dataset was evaluated using the coefficient of variation, skewness to examine asymmetrical distributions, and kurtosis to estimate the total weight of tails in light of the overall distribution (Animashaun et al., 2020).

2.3. Homogeneity tests

The homogeneity analysis of mean annual rainfall, maximum and minimum temperature datasets for each station was evaluated using Pettitt, von Neumann, SNHT, and Buishand tests. Using collected climate data for the meteorological station, the study examined the homogeneity tests, and the results p-value was compared with alpha ($\alpha=0.05$), if the p-value was greater than alpha, it indicates that it's homogenous with a 95% level of significance (Daba et al., 2020; Gulakhmadov et al., 2020; Bekele et al., 2023).

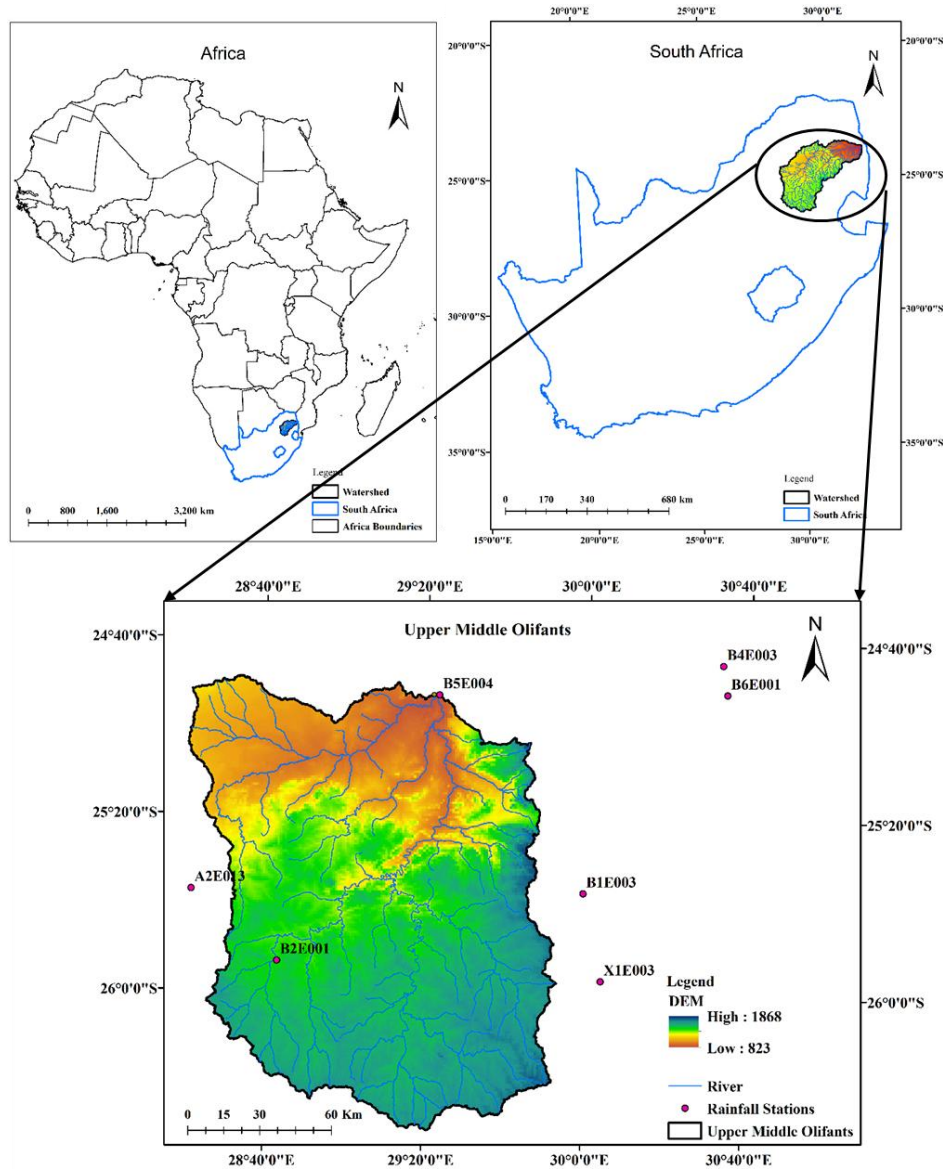


Figure 1. The location map of Africa, South Africa (Olifant River Basin), and Upper Middle Olifants Catchment

Pettitt Test

The Pettitt test is used to identify a shift or change point in time series data (Pettitt, 1979; Fentaw et al., 2019; Gulakhmadov et al., 2020). The test employs a modified Mann-Whitney, $U_{t,N}$ to determine if two sample sets X_1, \dots, X_t and X_{t+1}, \dots, X_N are all in the same population. The test statistic $U_{t,N}$ was computed using equations 1 to 4:

$$U_{t,N} = U_{t-1,N} + \sum_{j=1}^N \text{sgn}(X_t - X_j) \quad (1)$$

where $t = 2, 3, \dots, N$ and sgn function are given by:

$$\text{sgn}(x_i - x_j) = \begin{cases} 1 & \text{if } x_i - x_j > 0 \\ 0 & \text{if } x_i - x_j = 0 \\ -1 & \text{if } x_i - x_j < 0 \end{cases} \quad (2)$$

The test statistic measures the number of times a first-sample member outranks a second-sample member. The test statistic K_N and the related probability (P) were shown as follows:

$$K_N = \max_{1 \leq t \leq N} |U_{t,N}| \quad (3)$$

$$P \cong 2 \exp \left\{ \frac{-6(K_N)^2}{N^3 + N^2} \right\} \quad (4)$$

where P is the probability of recognising a point change. A significant change of point in the time

series data is defined as a 'P' value less than 0.05, with a 5% significance level to be used (Gulakhmadov et al., 2020). This study used the XLSTAT software to identify the shift in climate data at a 5% significance level.

Buishand Test

The Buishand test is a parametric technique and assumes that the data set is uniformly distributed or null, and the data's second hypothesis includes shifts (Buishand, 1982). Buishand's test was applied to variables based on the distributions (Buishand, 1982). Assume that $x_1 \dots x_m \dots x_n$ are observed time series with a mean (\bar{x}) and adjusted partial summation was computed by using equation 5:

$$S_m = \sum_{i=1}^m (x_i - \bar{x}) \quad (5)$$

If S_m oscillates about zero, the time series is homogeneous. Equation 6 was used to estimate the significant change in a time series (Buishand, 1982):

$$R = \frac{\text{Max}(S_m) - \text{Min}(S_m)}{\bar{x}} \quad (6)$$

SNHT

The SNHT is commonly used to compare a set of ratios to a mean value (Daba et al., 2020). The average of the first m years was compared to the average across the last n-m years using the Tm statistic as shown in equation 7 (Animashaun et al., 2020):

$$T_m = m\bar{z}_1 + (n - m)\bar{z}_2 \quad (7)$$

where s is the variance of the data, $\bar{z}_1 = \frac{1}{m} \sum_{i=1}^m \frac{(x_i - \bar{x})}{s}$ and $\bar{z}_2 = \frac{1}{n-m} \sum_{i=m+1}^n \frac{(x_i - \bar{x})}{s}$. The year m is the change point if the value of T_m is maximum. If the statistical result is higher than the critical value, which again is determined by the sample size n, then the null hypothesis should be rejected.

Von Neumann test

The Von Neumann test assesses the randomization and recognition of change points in time series data, and the test equation 8 is expressed as follows (Salehi et al., 2020):

$$N = \frac{\sum_{i=1}^{n-1} (x_i - x_{i-1})^2}{\sum_{i=1}^n (x_i - \bar{x})^2} \quad (8)$$

The time series is homogeneous if the expected value of N is 2; otherwise, the value of N is less

than 2, which shows a break (Kazemzadeh & Malekian, 2018).

2.4. Trend analysis

The Sen's slope and Mann-Kendall tests were used to detect the trend of the mean annual rainfall and temperature at each station in the study area (Asfaw et al., 2018; Adane et al., 2020). The non-parametric Mann-Kendall test indicates the trend based on the standard normal statistic (Z) results. If the Z is positive, negative, or zero, the trend is growing, declining, or the null hypothesis is accepted, respectively (Mann, 1945; Kendall, 1975; Gonfa et al., 2022; Nannawo et al., 2022). Sen's slope is frequently used to detect the magnitude and direction of trends in time series datasets and non-parametric data (Sen, 1968; Hussain et al., 2021). Positive or negative slope values indicate rising or declining trends, respectively (Nasir et al., 2021).

Mann-Kendall test

The existence of trends in time series data was examined using the Mann-Kendall (MK) test. MK is a rank-based, non-parametric test widely used to detect trends in time series in Ethiopia at the basin scale (Tekleab et al., 2014). The MK test is given as equation 9:

$$S = \sum_{k=1}^{n-1} \sum_{j=k+1}^n \text{Sgn}(x_j - x_k) \quad (9)$$

where x_i and x_k are observed data with $j > k$, and the sign function is given as equation 10:

$$\text{Sign}(x_j - x_k) = \begin{cases} 1 & \text{if } x_j - x_k > 0 \\ 0 & \text{if } x_j - x_k = 0 \\ -1 & \text{if } x_j - x_k < 0 \end{cases} \quad (10)$$

For identically distributed, independent data with no tied elements, the variance var (S) and the most expected value, E(S), of the distribution are presented in Equation 11:

$$\text{var}(S) = \frac{n(n-1)(2n+5)}{18} \quad (11)$$

$$E(S) = 0$$

If there is one or more tied (equal value), the standard deviation may be calculated as shown in Equation 13.

$$\text{VAR}(S) = \frac{n(n-1)(2n+5) - \sum_{k=1}^n t_k(k-1)(2k+5)}{18} \quad (13)$$

where n = number of data values; t_k is the number of tied elements of extent k. For a large sample size of over 10 data points, the standard normal test statistic was given as equation 14:

$$Z = \begin{cases} \frac{S-1}{\sqrt{\text{VAR}(S)}} & \text{if } S > 0 \\ 0 & \text{if } S = 0 \\ \frac{S+1}{\sqrt{\text{VAR}(S)}} & \text{if } S < 0 \end{cases} \quad (14)$$

The presence of a statistically significant trend is evaluated using the Z value at a 5% significance level. A positive Z indicates an increasing trend, and a negative value indicates a decreasing trend (when an alternative hypothesis H_1 is accepted). When the Z value equals zero, it shows neither an increasing nor a decreasing trend in the data series (when the null hypothesis, H_0 , is accepted).

Sen's slope test

Sen's slope has been frequently applied to estimate the magnitude of trends in time series data of climate variability of nonparametric data, and the Mann–Kendall test reveals the direction of significant trends, not the magnitude (Hussain et al., 2021). If there is a linear trend, the actual slope (shift in unit time) will be computed using Sen's slope, which uses equation 15 to estimate N pairs of data (Sen, 1968):

$$\varphi_i = \frac{(X_j - X_k)}{j - k} \text{ For } i = 1, 2, \dots, N \quad (15)$$

Where X_j and X_k are data at time j and k ($j > k$), and the median of these N values of φ_i is Sen's slope, which is described by equation 16:

$$\varphi_{med} = \begin{cases} \varphi_{(\frac{N+1}{2})} & \text{if } N \text{ is odd} \\ \frac{\varphi_{(\frac{N}{2})} + \varphi_{(\frac{N+2}{2})}}{2} & \text{if } N \text{ is even} \end{cases} \quad (16)$$

The φ_{med} sign denotes the reflection of data trends, whereas the value shows the steepness of the trend. The confidence interval φ_{med} at a given

probability should be obtained to evaluate whether the median slope is statistically distinct from zero. The Sen's slope (true slope) will be used to see a change in slope on the climatic and hydrological time series dataset in the Olifants River study area using the XLSTAT software. Positive or negative slope values indicate rising or declining trends, respectively (Nasir et al., 2021). Generally, the XLSTAT software statistical analysis package was used to check the homogeneity, Mann-Kendall, and Sen's slope tests.

3. Results and Discussion

3.1. Variability analysis

The statistical analysis was conducted to determine climate variability of mean annual rainfall and maximum and minimum temperatures for each station (Tables 1 and 2). The annual rainfall ranges from 690.21 to 837.13 mm for seven rainfall stations in the UMOC, with a significant variation of Standard Deviation (SD) (Table 1). However, the coefficient of variation (CV) results for stations such as X1E003, B5E004, and B1E003 show less variability ($CV < 20$), while the rest of the stations show moderate variation ranges ($20 < CV < 30$) (Animashaun et al., 2020). The annual rainfall was negatively skewed for stations such as X1E003 and B1E003, while the kurtosis depicts that X1E003, B4E003, A2E013, and B5E004 were not normally distributed (Table 1). In South Africa's Rietspruit sub-basin, the variation coefficient of annual rainfall is mainly categorized into moderate variation ranges (Banda et al., 2021).

Table 1. Variability analysis results for the annual rainfall

Statics	X1E003	B2E001	B4E003	A2E013	B6E001	B5E004	B1E003
Mean	725.96	690.21	811.80	690.50	720.35	580.90	837.13
SD	136.72	189.50	163.36	167.11	148.20	109.36	160.64
CV	18.83	27.45	20.12	24.20	20.57	18.83	19.19
Kurtosis	-0.38	1.10	-0.22	-0.02	0.00	-0.41	0.00
Skewness	-0.12	0.29	0.41	0.28	0.46	0.36	-0.06
Minimum	467.43	251.60	545.28	348.92	449.82	385.38	454.89
Maximum	987.43	1184.09	1176.56	1086.09	1045.23	824.48	1123.98

Moreover, annual maximum and minimum temperature findings show slight deviation and variability (Table 2). The maximum temperature for all stations was negatively skewed, while B6E001 was not normally distributed (Table 2).

Most stations were negatively skewed for annual minimum temperature assessment (Table 2). The X1E003 station's coefficient of variation was higher than that of other stations for both annual maximum and minimum temperatures. The study

covering South Africa's Eastern Cape, Gauteng, KwaZulu-Natal, Limpopo, and Mpumalanga provinces shows a considerable rainfall variability (Masingi & Maposa, 2021). Specifically, the rainfall variability was significant in the KwaZulu-Natal province (Ndlovu et al., 2021). The rainfall variability was also significantly high, while the maximum and minimum temperatures resulted in minimal variability in the Limpopo Province (Maluleke et

al., 2024). Numerous studies highlighted significant rainfall and temperature variability worldwide (Akbar & Gheewala, 2020; Jayasekara et al., 2020; Praveen et al., 2020). The results recorded were comparable to historical climate variability throughout Africa, in general, and specifically in South Africa (Animashaun et al., 2020; Banda et al., 2021; Mosase & Ahiablame, 2018; Bekele et al., 2023).

Table 2. Variability analysis results for the annual temperature

	Statistics	X1E003	B2E001	B4E003	A2E013	B6E001	B5E004	B1E003
Maximum Temperature	Mean	23.00	24.86	27.76	24.60	27.59	28.15	22.44
	SD	0.96	0.83	0.84	0.88	0.80	0.74	0.90
	CV	4.17	3.35	3.02	3.58	2.91	2.62	4.03
	Kurtosis	0.21	0.35	0.92	0.52	-0.03	0.58	0.45
	Skewness	-0.17	-0.43	-0.61	-0.34	-0.38	-0.32	-0.28
	Minimum	20.85	22.84	25.60	22.49	25.88	26.35	20.35
Maximum Temperature	Maximum	25.07	26.60	29.24	26.32	29.22	29.60	24.34
	Mean	8.36	9.80	13.86	12.27	11.25	12.99	8.46
	SD	0.42	0.41	0.41	0.43	0.39	0.42	0.39
	CV	5.04	4.19	2.96	3.49	3.46	3.20	4.67
	Kurtosis	1.48	0.92	0.24	0.92	0.83	1.30	1.61
	Skewness	0.14	0.11	-0.09	0.01	-0.10	-0.11	-0.18
Maximum Temperature	Minimum	7.28	8.85	12.94	11.29	10.27	12.01	7.38
	Maximum	9.43	10.81	14.74	13.31	12.15	14.02	9.39

3.2 Change point detection tests

Homogeneity analysis (change point detection) for annual rainfall, maximum and minimum temperature time series datasets was evaluated using Pettitt, Buishand, von Neumann, and SNHT. Surprisingly, the annual rainfall and maximum temperature homogeneity test results were greater than alpha ($\alpha=0.05$) for all meteorological stations (Tables 3 and 4). This means that the annual precipitation and maximum temperature are homogeneous and have not deviated much from the historical rising trend. However, the minimum annual temperature analyses that were categorized as not homogeneous were B4E003, B6E001, B5E004, and B1E003 for Pettitt; B6E001 for SHNT; and X1E003, B6E001, and B1E003 for Buishand tests (Table 4). The minimum temperature exhibited inhomogeneity in 1997 and 2002 for most of the tests and stations. Most

meteorological stations fall within defined homogeneous category ranges (Bekele et al., 2023). Like the Olifants River, most station rainfall and temperature data were homogenous in South Africa's Rietspruit sub-basin (Banda et al., 2021). Even though no study has clearly assessed the minimum temperature change point, increasing changes have been observed in the temperature pattern in the study area (Nkhonjera, 2017; Mosase & Ahiablame, 2018; Olabanji et al., 2020; Nkhonjera et al., 2021).

Table 3. Homogeneity test results for the annual rainfall

Station	Pettitt			SHNT			Buishand			von Neumann	
	K	t	p-value	T0	t	p-value	Q	t	p-value	N	p-value
X1E003	62	2005	0.46	2.66	2005	0.72	4.07	2005	0.48	2.95	0.99
B2E001	44	1994	0.81	5.56	2013	0.24	3.15	2000	0.73	1.74	0.21
B4E003	66	2009	0.40	3.13	2011	0.54	3.55	2009	0.69	1.63	0.21
A2E013	74	2005	0.24	3.27	1994	0.53	4.19	1994	0.31	1.86	0.32
B6E001	68	2009	0.30	3.61	2012	0.40	3.50	2009	0.57	1.61	0.14
B5E004	52	2005	0.64	1.90	1994	0.81	3.20	1994	0.74	1.85	0.37
B1E003	44	2000	0.84	0.96	2000	1.00	2.59	2000	0.93	2.16	0.65

Table 4. Variability analysis results for the annual temperature

		Pettitt			SHNT			Buishand			von Neumann	
		K	t	p-value	T0	t	p-value	Q	t	p-value	N	p-value
Maximum Temperature	X1E003	86	1997	0.12	3.90	2000	0.38	5.23	2000	0.14	1.87	0.42
	B2E001	82	1997	0.19	4.32	2000	0.44	5.50	2000	0.15	1.70	0.24
	B4E003	78	2000	0.15	4.03	2000	0.38	5.31	2000	0.13	1.46	0.07
	A2E013	88	2000	0.08	3.91	2000	0.37	5.23	2000	0.11	5.34	0.43
	B6E001	80	1997	0.22	3.49	2000	0.51	4.94	2000	0.24	1.91	0.45
	B5E004	74	1997	0.37	2.95	2000	0.67	4.54	2000	0.33	1.98	0.51
	B1E003	80	2000	0.13	2.96	2000	0.67	4.55	2000	0.32	5.17	0.59
Minimum Temperature	X1E003	90	1997	0.12	6.51	1997	0.21	6.52	1997	0.03	1.48	0.09
	B2E001	84	1997	0.11	5.47	2002	0.28	6.15	2002	0.09	1.50	0.06
	B4E003	106	1997	0.02	6.85	1997	0.13	6.69	1997	0.07	1.35	0.09
	A2E013	76	1997	0.14	4.75	2002	0.31	5.74	2002	0.06	1.72	0.29
	B6E001	118	1997	0.01	7.97	1997	0.02	7.22	1997	0.02	1.55	0.13
	B5E004	98	1997	0.04	6.60	1997	0.12	6.57	1997	0.05	1.57	0.14
	B1E003	108	1997	0.03	7.28	1997	0.14	6.90	1997	0.01	1.48	0.07

Note: An italicized p-value < 0.05 means the dataset is not homogeneous.

3.3. Trend analysis

In most of the stations in the Olifants River, annual rainfall exhibited increasing trends, except for B2E001 and B1E003 stations (Figure 2). Furthermore, the B2E001 station depicted a slightly decreasing trend based on Mann-Kendall (two-tailed test) and Sen's slope values (Table 5). Meanwhile, the B1E003 station's trend analysis showed no trend for both methods (Table 5). Furthermore, based on the statistics, the A2E013 station trend analysis results surpassed all stations. In the study area, the rainfall pattern has been increasing dramatically annually from 1979 to 2013 in South Africa's Limpopo River basin (Mosase & Ahiablame, 2018). Also, most Upper Karoo's rainfall stations show increasing trends from 1989 to 2018 (Harmse et al., 2021). Furthermore, there was no significantly increasing trend in South Africa's Rietspruit sub-basin (Banda et al., 2021). Using Sen's slope test,

the Limpopo River exhibited a rising rainfall trend except in Gwanda station (Nyikadzino et al., 2020). Additionally, rainfall variability considerably increased in most of the selected stations in Malawi, Mozambique, South Africa, and Zimbabwe (Mupangwa et al., 2021). Unlike the Southern Africa region, the rainfall pattern in the Horn of Africa showed a declining trend in most of the raingauge stations (Asfaw et al., 2018; Belihu et al., 2018; Mulugeta et al., 2019; Adane et al., 2020; Aredo et al., 2021a; Gurara et al., 2022). The annual maximum temperature trend analysis slightly increased in the Upper-Middle Olifants catchment (Table 6 and Figure 3). However, the annual minimum temperature was slightly increasing at stations such as X1E003, B2E001, A2E013, and B5E004, while it was moderately increasing at B4E003, B6E001, and B1E003 (Table 6 and Figure 4).

Table 5. Trend analysis for the annual rainfall

Station Number	Trend test			
	Kendall's tau	S	p-value	Sen's slope
X1E003	0.13	47	0.34	3.92
B2E001	-0.03	-11	0.84	-1.95
B4E003	0.09	31	0.54	2.43
A2E013	0.15	53	0.28	4.89
B6E001	0.08	29	0.56	2.24
B5E004	0.08	27	0.59	1.14
B1E003	0.00	-1.0	1.00	-0.07

Table 6. Trend analysis for the annual temperature

Station Number	Maximum Temperature				Minimum Temperature			
	Kendall's tau	S	p-value	Sen's slope	Kendall's tau	S	p-value	Sen's slope
X1E003	0.14	49	0.32	0.024	0.15	53	0.28	0.010
B2E001	0.15	51	0.3	0.025	0.15	51	0.3	0.011
B4E003	0.10	35	0.48	0.016	0.21	73	0.13	0.014
A2E013	0.12	43	0.39	0.018	0.13	45	0.36	0.010
B6E001	0.15	51	0.3	0.019	0.24	85	0.08	0.014
B5E004	0.08	29	0.56	0.009	0.17	61	0.21	0.011
B1E003	0.13	45	0.36	0.017	0.2	69	0.16	0.011

Increasing annual maximum and minimum temperatures have been increasing following the global climate change pattern and have been noticed in most African and the global south countries. For instance, in the Asian region, the trend analysis outcomes showed upward and downward trends for maximum and minimum temperature, respectively (Ali et al., 2019; Singh et al., 2020). The mean temperature in Africa's Lake Chad showed a considerably rising trend in historical datasets (Mahmood & Jia, 2019). Similarly, the annual maximum and minimum temperatures were observed in the Limpopo River Basin, resulting in an increasing trend during the study periods (Mosase & Ahiablame, 2018). Also, the findings of Kruger & Shongwe (2004) depict an increasing temperature trend in South Africa's numerous study areas. Furthermore, the future rainfall pattern showed significant variability and may pose a drought vulnerability in South Africa's Eastern Cape (Mahlalela et al., 2020). Comparable climate trend analysis observed in South Africa's Limpopo River Basin (Gebre & Getahun, 2016; Maluleke et al., 2024).

Furthermore, the climate variability and trend analysis study showed high unpredictability and

vulnerability to food insecurity in South Africa's Limpopo province (Shikwambana et al., 2021). There was a call for measures to mitigate South Africa's temperature and rainfall variability (Nsubuga et al., 2019). This study also emphasized the need for intervention to mitigate the ramifications of climate variability, which is consistent with the findings and previous studies conducted in South Africa. Moreover, the findings of this study will provide insight into the understanding of the Olifants River's historical climatic variability and trends in South Africa. Sustainable and innovative climate effects mitigation methods must be initiated to lessen the ramifications on agricultural productivity and environmental changes. Furthermore, boosting afforestation and water conservation activities to mitigate future climate effects will be imperative for the study area. Additionally, future studies could potentially explore the impact of natural and human activities on hydrology using physically based distributed models and considering coping strategies for likely hydrological extremes and water resources availability.

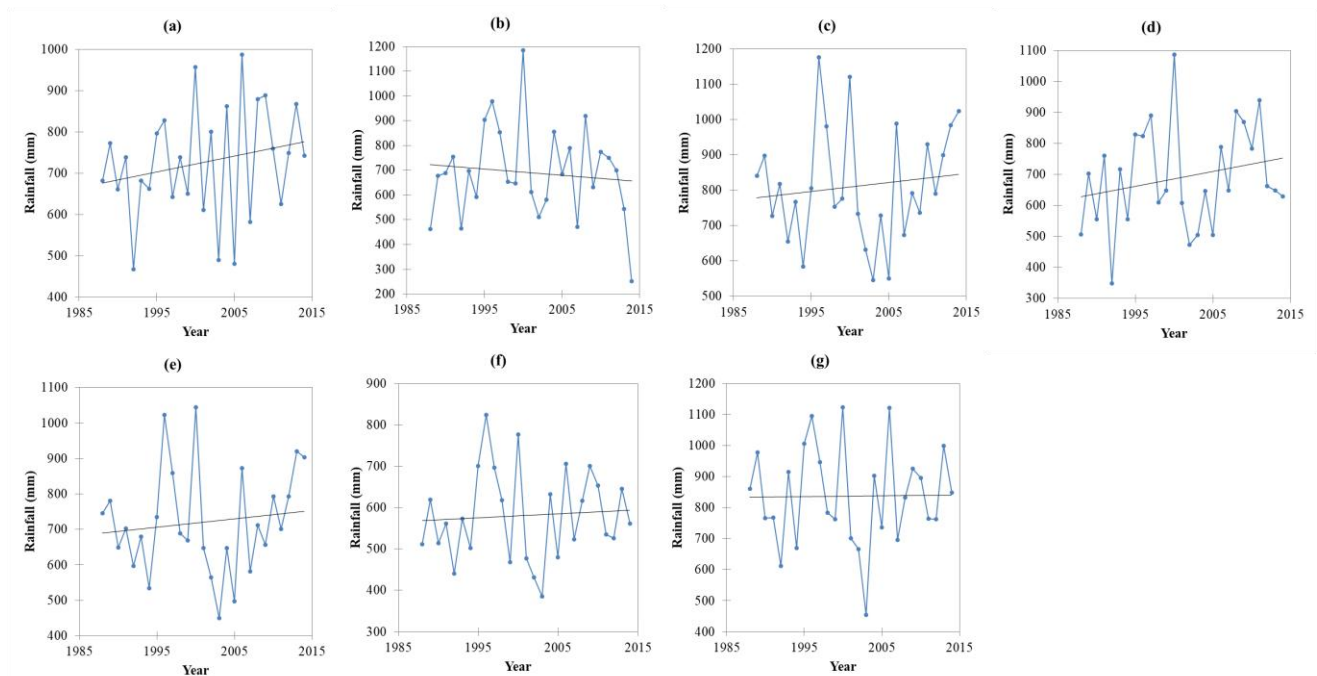


Figure 2. Mann-Kendall (two-tailed test) trend analysis for annual rainfall (mm): (a) X1E003, (b) B2E001, (c) B4E003, (d) A2E013, (e) B6E001, (f) B5E004, and (g) B1E003

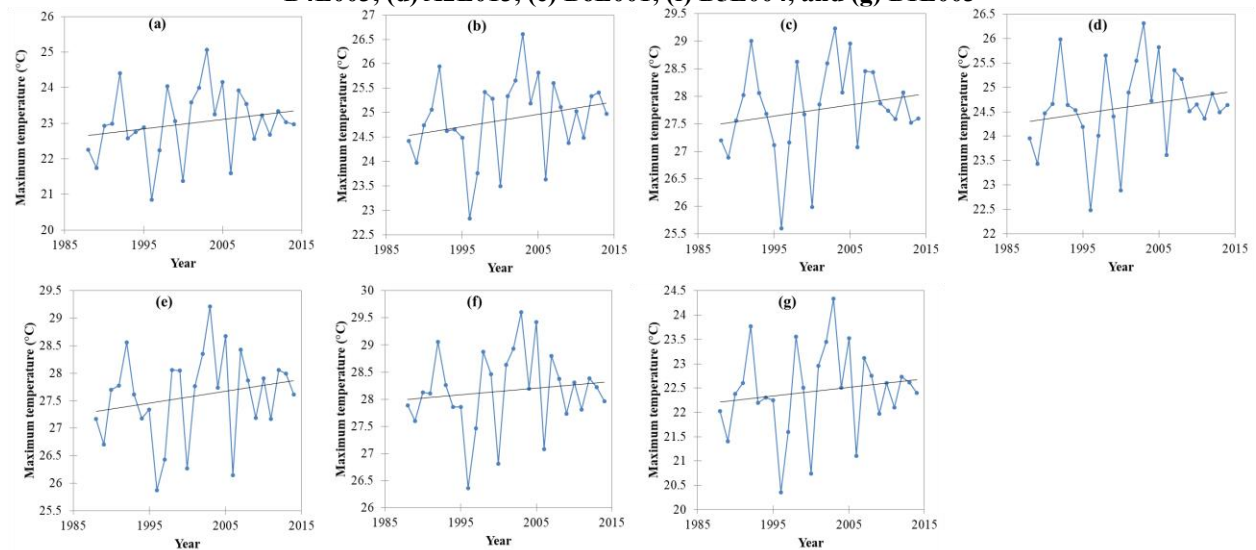


Figure 3. Mann-Kendall (two-tailed test) trend analysis for annual maximum temperature (°C): (a) X1E003, (b) B2E001, (c) B4E003, (d) A2E013, (e) B6E001, (f) B5E004, and (g) B1E003

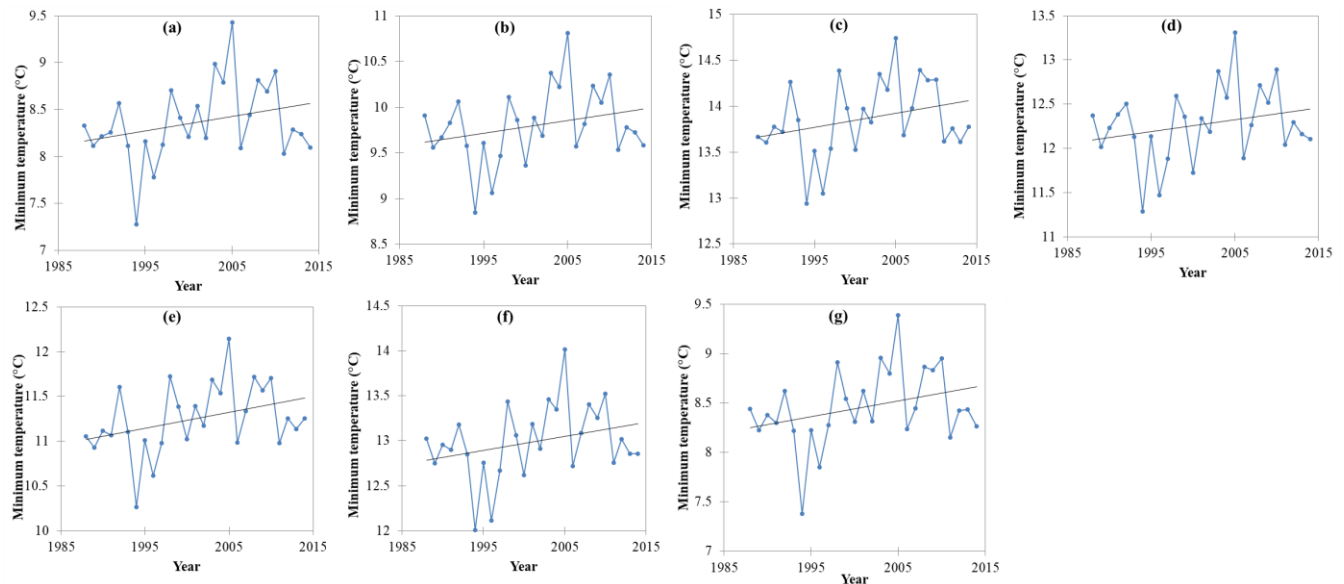


Figure 4. Mann- Mann-Kendall (two-tailed test) trend analysis for annual minimum temperature (°C): (a) X1E003, (b) B2E001, (c) B4E003, (d) A2E013, (e) B6E001, (f) B5E004, and (g) B1E003

4. Conclusions

The study examined the change point detection, trend, and variability analysis of temperature and rainfall time series datasets in the Olifants River (South Africa) using numerous statistical analysis methods from 1988 to 2014. The annual rainfall variability analysis showed that a few stations were negatively skewed; most stations were in moderate variations and not normally distributed. However, the annual temperature analysis depicts slightly deviated and varied results, while most stations were negatively skewed. Surprisingly, all stations' annual rainfall and maximum temperature datasets were homogeneous. Furthermore, most tests and stations' minimum temperature data reflect inhomogeneity in 1997 and 2002. The annual rainfall analysis has resulted in a rising trend, except for B2E001 (slightly dropping trend) and B1E003 (no trend) stations.

Additionally, the annual rainfall trend analysis showed disparities, while maximum and minimum temperatures showed an increasing trend with varying magnitudes. This study area is novel by enhancing the limited understanding of detection, climate variability, and trend analysis in the Olifants River basin. The outcome of this study will contribute to understanding water resources development and effective management. Moreover, this study is limited to study periods, and future studies can include

incorporating future climate change impact on water resources using physically-based distributed hydrological models in the Olifants River, South Africa. The stakeholders can boost the availability of water resources by implementing water conservation initiatives in the study area.

Acknowledgements:

The authors thank the South African Weather Services for providing the climate data. The authors are glad to thank the University of Johannesburg for its support in this research. We want to thank the editor and anonymous reviewers for taking their valuable time and constructive feedback, which helped boost this article's quality in the review process.

Author Contributions:

Mesfin Reta Aredo: Conceptualization, methodology, formal analysis and investigation, visualization, resources, writing-original draft preparation.

Megersa Olumana Dinka: Supervised, reviewed, and edited the manuscript.

Conflicts of interest

The authors of this article declared no conflict of interest regarding the authorship or publication of this article.

Data availability statement:

All data generated or analyzed during this study are included in this published article.

References

- Abera, E.A., Abegaz, W.B., 2020. Seasonal and Annual Rainfall Trend Detection in Eastern Amhara, Ethiopia. *Journal of Climatol Weather & Forecasting*, 8(3), 1–10. doi: 10.35248/2332-2594.2020.8.264
- Abungba, J.A., Khare, D., Pingale, S.M., Adjei, K.A., Gyamfi, C., Odai, S.N., 2020. Assessment of Hydro-climatic Trends and Variability over the Black Volta Basin in Ghana. *Earth Systems and Environment*, 4(4), 739–755. doi: 10.1007/s41748-020-00171-9
- Adane, G.B., Hirpa, B.A., Song, C., Lee, W.K., 2020. Rainfall characterization and trend analysis of wet spell length across varied landscapes of the Upper Awash River Basin, Ethiopia. *Sustainability*, 12(9221). doi: 10.3390/su12219221
- Adeola, A., Ncongwane, K., Abiodun, G., Makgoale, T., Rautenbach, H., Botai, J., Adisa, O., Botai, C., 2019. Rainfall trends and malaria occurrences in Limpopo province, South Africa. *International Journal of Environmental Research and Public Health*, 16(24). doi: 10.3390/ijerph16245156
- Akbar, H., Gheewala, S.H., 2020. Changes in hydroclimatic trends in the Kunhar River Watershed. *Journal of Sustainable Energy & Environment*, 11(June), 31–41. doi: 10.13140/RG.2.2.12517.42725
- Alashan, S., 2020. Combination of modified Mann-Kendall method and Sen innovative trend analysis. *Engineering Reports*, 2(3), 1–13. doi: 10.1002/eng2.12131
- Ali, R., Kuriqi, A., Abubaker, S., Kisi, O., 2019. Long-term trends and seasonality detection of the observed flow in Yangtze River using Mann-Kendall and Sen's innovative trend method. *Water (Switzerland)*, 11(9). doi: 10.3390/w11091855
- Animashaun, I. M., Oguntunde, P.G., Akinwumiju, A.S., Olubanjo, O.O., 2020. Rainfall Analysis over the Niger Central Hydrological Area, Nigeria: Variability, Trend, and Change point detection. *Scientific African*, 8(e00419). doi: 10.1016/j.sciaf.2020.e00419
- Aredo, M.R., Hatiye, S.D., Pingale, S.M., 2021a. Impact of land use/land cover change on stream flow in the Shaya catchment of Ethiopia using the MIKE SHE model. *Arabian Journal of Geosciences*, 14(114). doi: 10.1007/s12517-021-06447-2
- Aredo, M.R., Hatiye, S.D., Pingale, S.M., 2021b. Modeling the rainfall-runoff using MIKE 11 NAM model in Shaya catchment, Ethiopia. *Modeling Earth Systems and Environment*, 7, 2545–2551. doi: 10.1007/s40808-020-01054-8
- Aredo, M.R., Lohani, T.K., Mohammed, A.K., 2023a. Assessment of river response to water abstractions in the Weyib Watershed, Ethiopia. *International Journal of River Basin Management*, 23(1), 93–104. doi: 10.1080/15715124.2023.2248488
- Aredo, M.R., Lohani, T.K., Mohammed, A.K., 2023b. Numerical groundwater modelling under changing water abstraction in Weyib watershed, Ethiopia. *Cogent Engineering*, 10(2). doi: 10.1080/23311916.2023.2283297
- Aredo, M.R., Lohani, T.K., Mohammed, A.K., 2024a. Groundwater recharge estimation using WetSpa-M and MTBS leveraging from HydroOffice and WHAT tools for baseflow in Weyib watershed, Ethiopia. *Environmental Monitoring and Assessment*, 196(6). doi: 10.1007/s10661-024-12643-w
- Aredo, M.R., Lohani, T.K., Mohammed, A.K., 2024b. Revisiting the global weights of the integrated watershed health assessment framework and Weyib watershed health analysis : Ethiopia's policy prospects. *World Water Policy*, 10(3), 1–31. doi: 10.1002/wwp2.12205
- Asfaw, A., Simane, B., Hassen, A., Bantider, A., 2018. Variability and time series trend analysis of rainfall and temperature in northcentral Ethiopia: A case study in Woleka sub-basin. *Weather and Climate Extremes*, 19, 29–41. doi: 10.1016/j.wace.2017.12.002
- Ayivi, F., Jha, M.K., 2018. Estimation of water balance and water yield in the Reedy Fork-Buffalo Creek Watershed in North Carolina using SWAT. *International Soil and Water*

- Conservation Research, 6, 203–213. doi: 10.1016/j.iswcr.2018.03.007
- Bai, P., Liu, X., Liang, K., Liu, C., 2015. Comparison of performance of twelve monthly water balance models in different climatic catchments of China. *Journal of Hydrology*, 529, 1030–1040. doi: 10.1016/j.jhydrol.2015.09.015
- Bailey, R. T., Wible, T. C., Arabi, M., Records, R.M., Ditty, J., 2016. Assessing regional-scale spatio-temporal patterns of groundwater–surface water interactions using a coupled SWAT-MODFLOW model. *Hydrological Processes*, 30(23), 4420–4433. doi: 10.1002/hyp.10933
- Banda, V.D., Dzwauro, R.B., Singh, S.K., Kanyerere, T., 2021. Trend analysis of selected hydro-meteorological variables for the Rietspruit sub-basin, South Africa. *Journal of Water and Climate Change*, 12(7), 3099–3123. doi: 10.2166/wcc.2021.260
- Bartels, R.J., Black, A.W., Keim, B.D., 2019. Trends in precipitation days in the United States. *International Journal of Climatology*, 40(2), 1038–1048. doi: 10.1002/joc.6254
- Bekele, M., Mulugeta, T., Belete, D., Dananto, M., 2023. Trends in climatic and hydrological parameters in the Ajora - Woybo watershed, Omo - Gibe River basin, Ethiopia. *SN Applied Sciences*, 5(45). doi: 10.1007/s42452-022-05270-y
- Belihu, M., Abate, B., Tekleab, S., Bewket, W., 2018. Hydro-meteorological trends in the Gidabo catchment of the Rift Valley Lakes Basin of Ethiopia. *Physics and Chemistry of the Earth*, 104, 84–101. doi: 10.1016/j.pce.2017.10.002
- Buishand, T. A., 1982. Some methods for testing the homogeneity of rainfall records. *Journal of Hydrology*, 58(58), 11–27. doi: 10.1016/0022-1694(82)90066-X
- Bushira, K.M., Hernandez, J.R., 2019. MODFLOW-Farm Process Modeling for Determining Effects of Agricultural Activities on Groundwater Levels and Groundwater Recharge. *Journal of Soil and Groundwater Environment*, 24(5), 17–30. doi: 10.7857/JSGE.2019.24.5.017
- Cherinet, A.A., Yan, D., Wang, H., Song, X., Qin, T., Kassa, M. T., Girma, A., Dorjsuren, B., Gedefaw, M., Wang, H., Yadamjav, O., 2019. Climate Trends of Temperature, Precipitation and River Discharge in the Abbay River Basin in Ethiopia. *Journal of Water Resource and Protection*, 11(10), 1292–1311. doi: 10.4236/jwarp.2019.1110075
- Daba, M.H., Ayele, G.T., You, S., 2020. Long-Term Homogeneity and Trends of Hydroclimatic Variables in Upper Awash River Basin, Ethiopia. *Advances in Meteorology*, 2020(1), 8861959. doi: 10.1155/2020/8861959
- Erena, S. H., Worku, H., 2019. Urban flood vulnerability assessments: the case of Dire Dawa city, Ethiopia. *Natural Hazards*, 97(2), 495–516. doi: 10.1007/s11069-019-03654-9
- Fentaw, F., Melesse, A.M., Hailu, D., Nigussie, A., 2019. Precipitation and streamflow variability in Tekeze River basin, Ethiopia. In *Extreme hydrology and climate variability* (pp. 103–121). Elsevier Inc. doi: 10.1016/B978-0-12-815998-9.00010-5
- Gao, F., Wang, Y., Chen, X., Yang, W., 2020. Trend analysis of rainfall time series in Shanxi province, Northern China (1957–2019). *Water (Switzerland)*, 12(9), 1–22. doi: 10.3390/W12092335
- Gebre, S.L., Getahun, Y.S., 2016. Analysis of Climate Variability and Drought Frequency Events on Limpopo River Basin, South Africa. *Hydrology Current Research*, 7(3). doi: 10.4172/2157-7587.1000249
- Gedefaw, M., Yan, D., Wang, H., Qin, T., Girma, A., Abiyu, A., Batsuren, D., 2018. Innovative trend analysis of annual and seasonal rainfall variability in Amhara Regional State, Ethiopia. *Atmosphere*, 9(326). doi: 10.3390/atmos9090326
- Gonfa, K.H., Alamirew, T., Melesse, A.M., 2022. Hydro-Climate Variability and Trend Analysis in the Jemma. *Hydrology*, 9(12), 209. doi: 10.3390/hydrology9120209
- Gulakhmadov, A., Chen, X., Gulakhmadov, N., Liu, T., Davlyatov, R., Sharofiddinov, S., Gulakhmadov, M., 2020. Long-term hydro-climatic trends in the mountainous Kofarnihon river Basin in Central Asia. *Water*, 12(8). doi: 10.3390/W12082140
- Gurara, M.A., Tolche, A.D., Jilo, N.B., Kassa, A.K., 2022). Annual and seasonal rainfall

- trend analysis using gridded dataset in the Wabe Shebele River Basin, Ethiopia. *Theoretical and Applied Climatology*, 150, 263–281. doi: 10.1007/s00704-022-04164-8
- Hadi, S.J., Tombul, M., 2018. Comparison of Spatial Interpolation Methods of Precipitation and Temperature Using Multiple Integration Periods. *Journal of the Indian Society of Remote Sensing*, 46(7), 1187–1199. doi: 10.1007/s12524-018-0783-1
- Harmse, C.J., Du Toit, J.C.O., Swanepoel, A., Gerber, H.J., 2021. Trend analysis of long-term rainfall data in the Upper Karoo of South Africa. *Transactions of the Royal Society of South Africa*, 76(1), 1–12. doi: 10.1080/0035919X.2020.1834467
- Hussain, A., Cao, J., Hussain, I., Begum, S., Akhtar, M., Wu, X., Guan, Y., Zhou, J., 2021. Observed Trends and Variability of Temperature and Precipitation and Their Global Teleconnections in the Upper Indus Basin, Hindukush-Karakoram-Himalaya. *Atmosphere*, 12(973). doi: 10.3390/atmos12080973
- Igibah, C.E., Tanko, J.A., 2019. Assessment of urban groundwater quality using Piper trilinear and multivariate techniques: a case study in the Abuja, North-central, Nigeria. *Environmental Systems Research*, 8(14). doi: 10.1186/s40068-019-0140-6
- Jayasekara, S., Abeysingha, N., Meegastenna, T., 2020. Streamflow trends of Kelani river basin in Sri Lanka (1983-2013). *Journal of the National Science Foundation of Sri Lanka*, 48(4), 449. doi: 10.4038/jnsfsr.v48i4.9440
- Jung, H.C., Getirana, A., Policelli, F., McNally, A., Arsenault, R., Kumar, S., Tadesse, T., & Peters-lidard, C.D., 2017. Upper Blue Nile Basin Water Budget from a Multi-Model Perspective. *Journal of Hydrology*, 555, 535–546. doi: 10.1016/j.jhydrol.2017.10.040
- Kazemzadeh, M., Malekian, A., 2018. Homogeneity analysis of streamflow records in arid and semi-arid regions of northwestern Iran. *Journal of Arid Land*, 10, 493–506 (2018). doi: 10.1007/s40333-018-0064-4
- Kendall, M.G., 1975. *Rank Correlation Methods*. 4th Edition, Charles Griffin, London.
- Kruger, A.C., Shongwe, S., 2004. Temperature trends in South Africa: 1960-2003. *International Journal of Climatology*, 24(15), 1929–1945. doi: 10.1002/joc.1096
- Loliyana, V.D., Patel, P.L., 2018. Performance evaluation and parameters sensitivity of a distributed hydrological model for a semi-arid catchment in India. *Journal of Earth System Science*, 127(117). doi: 10.1007/s12040-018-1021-5
- Mahlalela, P.T., Blamey, R.C., Hart, N.C.G., Reason, C.J.C., 2020. Drought in the Eastern Cape region of South Africa and trends in rainfall characteristics. *Climate Dynamics*, 55(9–10), 2743–2759. doi: 10.1007/s00382-020-05413-0
- Mahmood, R., Jia, S., 2019. Assessment of hydro-climatic trends and causes of dramatically declining stream flow to Lake Chad, Africa, using a hydrological approach. *Science of the Total Environment*, 675, 122–140. doi: 10.1016/j.scitotenv.2019.04.219
- Makungo, R., Odiyo, J.O., Ndiritu, J.G., Mwaka, B., 2010. Rainfall-runoff modelling approach for ungauged catchments: A case study of Nzhelele River sub-quaternary catchment. *Physics and Chemistry of the Earth*, 35, 596–607. doi: 10.1016/j.pce.2010.08.001
- Maluleke, P., Moeletsi, M.E., Tsubo, M., 2024. Analysis of Climate Variability and Its Implications on Rangelands in the Limpopo Province. *Climate*, 12(2). doi: 10.3390/cli12010002
- Mann, H.B., 1945. Nonparametric Tests Against Trend. *Econometrica*, 13(3), 245–259. doi: 10.2307/1907187
- Masingi, V.N., Maposa, D., 2021. Modelling long-term monthly rainfall variability in selected provinces of South Africa: Trend and extreme value analysis approaches. *Hydrology*, 8(70), 1–27. doi: 10.3390/hydrology8020070
- Mosase, E., Ahiablame, L., 2018. Rainfall and temperature in the Limpopo River Basin, Southern Africa: Means, variations, and trends from 1979 to 2013. *Water (Switzerland)*, 10(4). doi: 10.3390/w10040364
- Mulugeta, S., Fedler, C., Ayana, M., 2019. Analysis of long-term trends of annual and seasonal rainfall in the Awash River Basin,

- Ethiopia. Water (Switzerland), 11(7). doi: 10.3390/w11071498
- Mupangwa, W., Makanza, R., Chipindu, L., Moeletsi, M., Mkuhlani, S., Liben, F., Nyagumbo, I., Mutenje, M., 2021. Temporal rainfall trend analysis in different agro-ecological regions of southern Africa. *Water SA*, 47(4), 466–479. doi: 10.17159/WSA/2021.V47.I4.3844
- Nannawo, A.S., Lohani, T.K., Eshete, A.A., Ayana, M.T., 2022. Evaluating the dynamics of hydroclimate and streamflow for data - scarce areas using MIKE11 - NAM model in Bilate river basin , Ethiopia. *Modeling Earth Systems and Environment*, 8(4), 4563–4578. doi: 10.1007/s40808-022-01455-x
- Nasir, J., Assefa, E., Zeleke, T., Gidey, E., 2021. Meteorological Drought in Northwestern Escarpment of Ethiopian Rift Valley: detection seasonal and spatial trends. *Environmental Systems Research*, 10(1). doi: 10.1186/s40068-021-00219-3
- Ndlovu, M., Clulow, A.D., Savage, M.J., Nhamo, L., Magidi, J., Mabhaudhi, T., 2021. An assessment of the impacts of climate variability and change in Kwazulu-Natal province, South Africa. *Atmosphere*, 12(4). doi: 10.3390/atmos1204042
- Nkhonjera, G. K., 2017. Understanding the impact of climate change on the dwindling water resources of South Africa, focusing mainly on Olifants River basin: A review. *Environmental Science and Policy*, 71, 19–29. doi: 10.1016/j.envsci.2017.02.004
- Nkhonjera, G.K., Dinka, M.O., Woyessa, Y.E., 2021. Assessment of localized seasonal precipitation variability in the upper middle catchment of the olifants river basin. *Journal of Water and Climate Change*, 12(1), 250–264. doi: 10.2166/wcc.2020.187
- Nsubuga, F.N.W., Mearns, K.F., Adeola, A.M., 2019. Lake Sibayi variations in response to climate variability in northern KwaZulu-Natal, South Africa. *Theoretical and Applied Climatology*, 137(1–2), 1233–1245. doi: 10.1007/s00704-018-2640-0
- Nyikadzino, B., Chitakira, M., Muchuru, S., 2020. Rainfall and runoff trend analysis in the Limpopo river basin using the Mann Kendall statistic. *Physics and Chemistry of the Earth*, 117(102870). doi: 10.1016/j.pce.2020.102870
- Olabanji, M.F., Ndarana, T., Davis, N., Archer, E., 2020. Climate change impact on water availability in the olifants catchment (South Africa) with potential adaptation strategies. *Physics and Chemistry of the Earth*, 120, 1–32. doi: 10.1016/j.pce.2020.102939
- Pathak, S., Ojha, C.S.P., Shukla, A.K., Garg, R.D., 2019. Assessment of Annual Water-Balance Models for Diverse Indian Watersheds. *Journal of Sustainable Water in the Built Environment*, 5(3). doi: 10.1061/jswbay.0000881
- Pettitt, A.N., 1979. A Non-parametric to the Approach Problem. *Journal of the Royal Statistical Society*, 28(2), 126–135.
- Pirani, F.J., Modarres, R., 2020. Geostatistical and deterministic methods for rainfall interpolation in the Zayandeh Rud basin, Iran. *Hydrological Sciences Journal*, 65(16), 2678–2692. doi: 10.1080/02626667.2020.1833014
- Praveen, B., Talukdar, S., Shahfahad, Mahato, S., Mondal, J., Sharma, P., Islam, A. R.M.T., Rahman, A., 2020. Analyzing trend and forecasting of rainfall changes in India using non-parametrical and machine learning approaches. *Scientific Reports*, 10(1), 1–21. doi: 10.1038/s41598-020-67228-7
- Salehi, S., Dehghani, M., Mortazavi, S.M., Singh, V.P., 2020. Trend analysis and change point detection of seasonal and annual precipitation in Iran. *International Journal of Climatology*, 40(1), 308–323. doi: 10.1002/joc.6211
- Sen, P.K., 1968. Estimates of the Regression Coefficient Based on Kendall 's Tau. *Journal of the American Statistical Association*, 63(324), 1379–1389. doi: 10.1080/01621459.1968.10480934
- Shahid, M., Rahman, K.U., 2021. Identifying the Annual and Seasonal Trends of Hydrological and Climatic Variables in the Indus Basin Pakistan. *Asia-Pacific Journal of Atmospheric Sciences*, 57(2), 191–205. doi: 10.1007/s13143-020-00194-2
- Shikwambana, S., Malaza, N., Shale, K., 2021. Impacts of rainfall and temperature changes on smallholder agriculture in the Limpopo province, South Africa. *Water*, 13(20). doi: 10.3390/w13202872

- Singh, L., Khare, D., Prabhash, K.M., Pingale, S.M., Thakur, H.P., 2020. Spatial and temporal precipitation trends of proposed smart cities based on homogeneous monsoon regions across India. *Journal of Water and Land Development*, 47(1), 150–159. doi: 10.24425/jwld.2020.135042
- Singh, R., Pandey, V.P., Kayastha, S.P., 2021. Hydro-climatic extremes in the Himalayan watersheds: a case of the Marshyangdi Watershed, Nepal. *Theoretical and Applied Climatology*, 143(1–2), 131–158. doi: 10.1007/s00704-020-03401-2
- Sinha, J., Sharma, A., Khan, M., Goyal, M.K., 2018. Assessment of the impacts of climatic variability and anthropogenic stress on hydrologic resilience to warming shifts in Peninsular India. In *Scientific Reports* (Vol. 8, Issue 1). Springer US. doi: 10.1038/s41598-018-32091-0
- Solaimani, K., Habaibnejad, M., Pirnia, A., 2021. Temporal trends of hydro-climatic variables and their relevance in water resource management. *International Journal of Sediment Research*, 36, 63–75. doi: 10.1016/j.ijsrc.2020.04.001
- Tadese, M.T., Kumar, L., Koech, R., Zemadim, B., 2019. Hydro-climatic variability: A characterisation and trend study of the Awash River Basin, Ethiopia. *Hydrology*, 6(35). doi: 10.3390/hydrology6020035
- Tefera, A.H., 2017. Application of Water Balance Model Simulation for Water Resource Assessment in Upper Blue Nile of North Ethiopia Using HEC-HMS by GIS and Remote Sensing: Case of Beles River Basin. *International Journal of Hydrology*, 1(7), 222–227. doi: 10.15406/ijh.2017.01.00038
- Tekleab, S., Mohamed, Y., Uhlenbrook, S., 2013. Hydro-climatic trends in the Abay/Upper Blue Nile basin, Ethiopia. *Physics and Chemistry of the Earth*, 61, 32–42. doi: 10.1016/j.pce.2013.04.017
- Tekleab, S., Mohamed, Y., Uhlenbrook, S., Wenninger, J., 2014. Hydrologic responses to land cover change: The case of Jedeb mesoscale catchment, Abay/Upper Blue Nile Basin, Ethiopia. *Hydrological Processes*, 28(20), 5149–5161. doi: 10.1002/hyp.9998
- Teshome, F.T., Bayabil, H.K., Thakural, L.N., Welidehanna, F.G., 2020. Verification of the MIKE11-NAM Model for Simulating Streamflow. *Journal of Environmental Protection*, 11, 152–167. doi: 10.4236/jep.2020.112010
- Thapa, B.R., Ishidaira, H., Pandey, V.P., Shakya, N.M., 2017. A multi-model approach for analyzing water balance dynamics in Kathmandu Valley, Nepal. *Journal of Hydrology: Regional Studies*, 9, 149–162. doi: 10.1016/j.ejrh.2016.12.080
- Wakigari, S.A., 2017. Evaluation of conceptual hydrological models in data scarce region of the upper blue Nile basin: Case of the upper guder catchment. *Hydrology*, 4(59). doi: 10.3390/hydrology4040059
- Zhao, F., Zhang, L., Chiew, F.H.S., Vaze, J., Cheng, L., 2013. The effect of spatial rainfall variability on water balance modelling for south-eastern Australian catchments. *Journal of Hydrology*, 493, 16–29. doi: 10.1016/j.jhydrol.2013.04.028